

# High concentration Yb-Er co-doped phosphate glass for optical fiber amplification

Nadia Giovanna Boetti<sup>1</sup>, Gerardo Cristian Scarpignato<sup>1</sup>, Joris Lousteau<sup>2</sup>, Diego Pugliese<sup>1</sup>, Lionel Bastard<sup>3</sup>, Jean-Emmanuel Broquin<sup>3</sup> and Daniel Milanese<sup>1</sup>

<sup>1</sup>Dipartimento di Scienza Applicata e Tecnologia—DISAT, Politecnico di Torino, Corso Duca delle Abruzzi 24, 10129 Torino, Italy

<sup>2</sup>Istituto Superiore Mario Boella, Via P. Boggio 61, 10138 Torino, Italy

<sup>3</sup>Univ. Grenoble Alpes, and CNRS, IMEP-LAHC, F-38000 Grenoble, France

E-mail: [nadia.boetti@polito.it](mailto:nadia.boetti@polito.it)

## Abstract

We present the fabrication and characterization of two high concentration Yb<sup>3+</sup>-Er<sup>3+</sup> co-doped double clad phosphate glass optical fibers (named A and B for short) manufactured by preform drawing, with the preform being obtained by the rod-in-tube technique. Optical amplification was demonstrated by core pumping 27 mm of fiber A (7/25/70  $\mu\text{m}$  and NA = 0.17 between core and inner cladding) with a laser diode at 976 nm, achieving a 10.7 dB internal gain, i.e., 4.0 dB cm<sup>-1</sup>, for small signal input at 1535 nm. Amplification was also demonstrated in a cladding-pumped counter propagating configuration using both fibers A and B (12/48/140  $\mu\text{m}$  and NA = 0.08). A maximum internal gain of 18.5 dB was achieved with 8 cm of fiber B, corresponding to an amplification of 2.3 dB cm<sup>-1</sup>, for small signal input at 1535 nm.

Keywords: optical fiber amplifier, double clad fiber, optical fiber fabrication, phosphate glass, Yb-Er co-doped fiber

## 1. Introduction

In recent years, the exploitation of short-pulse fiber-based laser sources has found numerous applications in industrial and scientific fields. The fiber format offers compactness, high beam quality through a single-mode regime and efficient thermal management, leading to high laser reliability and stability. However, nonlinear optical effects due to the combination of high optical intensity in the single-mode fiber and long fiber amplifier length tend to impair considerably the temporal pulse properties and therefore prevents the achievement of high peak power in fiber-based pulsed laser sources [1].

Recently, tremendous efforts focused on well advanced silica glass fiber technology have been engaged for developing new types of fiber able to overcome the previously mentioned limitations. Different strategies have been implemented. Of particular note are large mode area fiber [2, 3] and

rod type fiber [4] whereby microstructured waveguide geometries have allowed us to achieve very low numerical aperture (NA) and thus to increase the core dimension while maintaining single-mode behavior and high beam quality. An additional advantage of this strategy is that it allows us to reduce the necessary fiber length. Also, a more subtle approach has been developed based on photonic bandgap fiber design [5].

In spite of these technological advancements, further improvements are still required. At the root of this technical bottleneck lies the low rare-earth (RE) ion doping concentration achievable in silica glass.

In recent years, phosphate glasses have attracted increasing interest as host media for RE-doped optical fibers. In fact, this glass system enables high concentration of RE ions (up to 10<sup>21</sup> ions/cm<sup>3</sup>) to be dissolved in the glass matrix without clustering, thanks to the presence of phosphorus, which introduces nonbridging oxygens in the structure, thus

resulting in an open, chain-like structure, compared to the random network of silicate glasses [6]. This allows the fabrication of compact active devices with high gain per unit length based on phosphate glasses [6]. Moreover this glass system possesses a large glass formation region, good thermomechanical and chemical properties, low nonlinear refractive index and no evidence of photodarkening even at high population inversion [8, 9].

Phosphate glass is recognized as an ideal host for an  $\text{Yb}^{3+}$ - $\text{Er}^{3+}$  co-doped system because of its high emission cross-section, low back energy transfer rate and low accumulative energy transfer rates [10]. In addition, the energy transfer efficiency from  $\text{Yb}^{3+}$  to  $\text{Er}^{3+}$  in phosphate glasses can be as high as 95% due to the large spectral overlap between the  $\text{Yb}^{3+}$  emission spectrum ( ${}^2\text{F}_{5/2} \rightarrow {}^2\text{F}_{7/2}$ ) and  $\text{Er}^{3+}$  absorption spectrum ( ${}^4\text{I}_{15/2} \rightarrow {}^4\text{I}_{11/2}$ ) [11].

$\text{Yb}^{3+}$ - $\text{Er}^{3+}$  phosphate glass fibers have been used to realize erbium-doped fiber amplifiers (EDFA) [12, 13] and compact narrow line-width fiber lasers [14–17] for telecommunications, interferometers and sensing instruments.

Attempts to combine the RE high solubility of phosphate glass and the ruggedness of silica fibers were made through the fabrication of phosphosilicate fibers, in which the incorporation of phosphorus in the glass matrix results in a more open structure that accounts for the higher solubility of dopants than in silica [18].

Nevertheless, it is most likely in the field of high energy, high average and peak power fiber optical amplification in which phosphate glasses can be a key enabler for a variety of optical devices. Indeed, they are an ideal medium for engineering the second stage of a master oscillator power amplifier (MOPA) fiber laser, thanks to their ability to maximize energy extraction and minimize the nonlinearities [19, 20]. It is worth noting that phosphate glass fibers can be also spliced to silica-based components with low loss and high strength, enabling the realization of a monolithic all-fiber MOPA system.

Recently phosphates have been also proposed as high-efficiency media for the realization of a novel monolithic fiber chirped pulse amplification system for high-energy femtosecond pulse generation [21].

Such potential applications have driven significant effort in the research activity of the proper host material composition, the optimum ratio of  $\text{Yb}^{3+}/\text{Er}^{3+}$  ions doping concentration, the suitable optical fiber geometry and the most appropriate preform and fiber fabrication technique. Nonetheless, further investigations and optimizations will broaden the opportunity for exploitation and new application fields.

In this paper we report on the fabrication and characterization of  $\text{Yb}^{3+}$ - $\text{Er}^{3+}$  co-doped double cladding (DC) phosphate glass optical fibers with reduced first cladding dimension for improving the pump absorption over a short length of fiber. To this end, several glass compositions were engineered, offering NA of 0.4 between the first and second cladding and NA as low as 0.08 between the core and the first cladding. As a preliminary assessment, we also report on the amplification operation of the fabricated fibers in the continuous wavelength regime.

## 2. Experimental

### 2.1. Fiber fabrication and characterization

A phosphate host glass ( $\text{P}_2\text{O}_5$ — $\text{Li}_2\text{O}$ — $\text{Al}_2\text{O}_3$ — $\text{BaO}$ — $\text{MgO}$ — $\text{La}_2\text{O}_3$ ) was ad hoc developed for this research in order to have a stable and robust glass able to incorporate a high amount of RE and that was suitable for fiber drawing. Based on this glass composition, three different glasses (core, inner cladding and outer cladding) were synthesized and characterized with the aim of fabricating  $\text{Yb}^{3+}$ - $\text{Er}^{3+}$  co-doped DC optical fibers. These glasses were designed in order to obtain the suitable refractive index contrast and therefore the desired NA between the core and inner cladding and between the inner cladding and outer cladding. In particular, the decrease of the refractive index in the two claddings was obtained by progressively increasing the amount of  $\text{Li}_2\text{O}$  and  $\text{MgO}$ , while decreasing  $\text{BaO}$  and  $\text{La}_2\text{O}_3$  content.

The chemicals were weighted and mixed inside a glove box under dried air atmosphere, then transferred into an alumina crucible for melting in a furnace at 1400 °C. A mix of  $\text{O}_2/\text{N}_2$  gases was purged into the furnace during melting in order to minimize the hydroxyl ions ( $\text{OH}^-$ ) content. The melt was then cast into a brass mold preheated at  $T_g-10^\circ\text{C}$  and annealed at the same temperature for 10 h. The core glass was doped with 2.79 wt% of  $\text{Er}_2\text{O}_3$  (1.08 mol%,  $2.9 \cdot 10^{20}$  ions/ $\text{cm}^3$ ) and 2.87 wt% of  $\text{Yb}_2\text{O}_3$  (1.08 mol%,  $2.9 \cdot 10^{20}$  ions/ $\text{cm}^3$ ). The RE ions concentrations were calculated from their initial compositions and measured sample densities, obtained by the Archimedes method using distilled water as an immersion fluid.

The fibers realized for this research were manufactured by preform drawing, with the preforms being obtained by the rod-in-tube technique. The fabrication of each preform required one rod of core glass fabricated by melt quenching and two cladding tubes shaped by rotational casting (at a rotation speed of 3000 rpm) using in-house-developed equipment. This process, initially developed for fluoride glass preform fabrication, was recently used by our research group on phosphate glasses: it proved to be a fast and reliable method for making tubes with an internal surface roughness rms value of 10 nm.

Figure 1 provides a schematic representation of the steps that were required in order to obtain the final DC preform that was used in the drawing process. The first step was the stretching of the core rod by cane drawing in order to fit inside the inner cladding tube. Both components were then combined to form an intermediate preform. The obtained core/inner cladding structure was finally stretched and placed in the outer cladding tube.

Fiber drawing was then carried out using a drawing tower developed in house. The furnace consists of a graphite ring heated by induction operating at 248 kHz and delivering 170 W to reach the drawing temperature (SAET, Torino, Italy).

The preform and fiber fabrication parameters were set to generate a DC fiber with the desired diameters. In particular, for this research two different DC optical fibers were

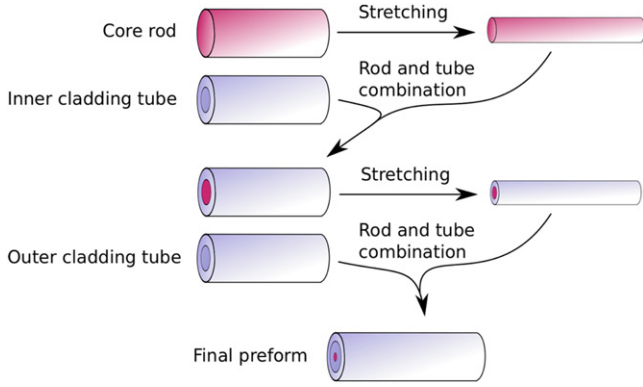


**Figure 1.** Schematic representation of main steps used for DC preform fabrication by rod-in-tube technique.

produced: fiber A with small dimensions and high NA between the core and inner cladding, and fiber B with opposite characteristics. Specifically, fiber A showed diameters of  $7\ \mu\text{m}$ ,  $25\ \mu\text{m}$  and  $70\ \mu\text{m}$  for the core, inner and outer cladding, respectively, with an NA between the core and inner cladding of 0.17. Fiber B, instead, showed diameters of  $12\ \mu\text{m}$ ,  $48\ \mu\text{m}$  and  $140\ \mu\text{m}$  for the core, inner and outer cladding, respectively, with an NA between the core and inner cladding of 0.08. Estimated error on fiber diameters was  $\pm 2\%$ .

The quality and morphology of the fabricated optical fibers were inspected by means of a Nikon ECLIPSE E 50i optical microscope. Fibers losses were measured by the cut-back technique using a length of about 300 cm with a single-mode fiber pigtailed laser diode source at 1300 nm. The laser was butt-coupled to one of the active fiber ends. The attenuation value was calculated through linear least square fitting of the experimental data.

The fibers' modal properties were investigated by taking a set of near-field images of the fiber cross-section, on a 280 cm-long fiber piece, at the wavelength of 1300 nm, using a butt-coupled fiber pigtailed laser diode source.

## 2.2. Core-pumped amplifier evaluation setup

Figure 2 shows the experimental setup employed for optical amplification measurement on 27 mm-long piece of active fiber A ( $7/25/70\ \mu\text{m}$ ) in core-pumped scheme. The optical pump at 976 nm was provided by a single-mode laser diode (1999CHP, 3SGroup) with a maximum power of around 500 mW. The optical signal ranging from 1500 to 1600 nm, with output power levels from  $-30\ \text{dBm}$  up to  $+5\ \text{dBm}$ , was obtained from a tunable laser (HP8168F). Both signal and pump were sent to the inputs of a Wavelength Division Multiplexer (WDM9890-250-A-1, Go4fiber), while the output was butt-coupled to the active fiber. The amplified signal was then collected by a fiber pigtail and sent to the entrance of an optical spectrum analyzer (Agilent 96140B).

In order to prevent any spurious laser emission, all measurements performed in this configuration were carried out using refractive index matching gel applied at both ends of the phosphate glass fiber. The gel improved also the coupling efficiency between butt-coupled fibers and contributed

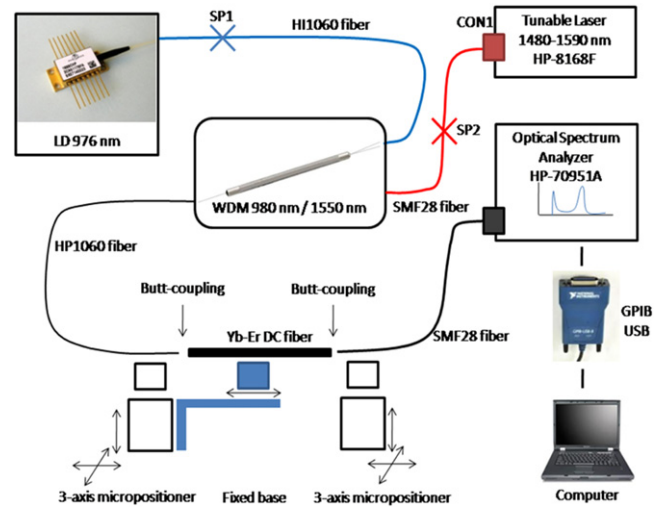


**Figure 2.** Experimental setup employed for the  $\text{Yb}^{3+}\text{-Er}^{3+}$  fiber amplifier characterization in a core-pumped configuration.

to the mechanical stability of the measurement by maintaining the fibers' correct alignment.

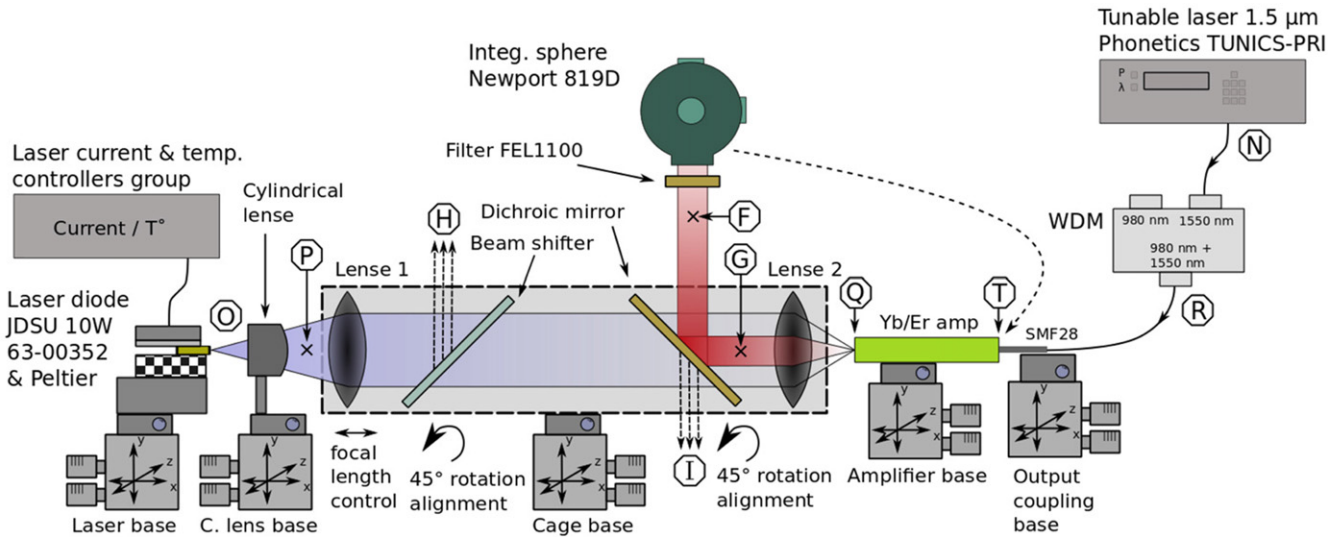
## 2.3. Cladding-pumped amplifier evaluation setup

Figure 3 depicts the schematic of the workbench used for the optical amplification measurement of an 8 cm-long active fiber B ( $12/48/140\ \mu\text{m}$ ) and 12 cm-long fiber A ( $7/25/70\ \mu\text{m}$ ) in a cladding-pumped scheme. A counter-propagating arrangement was employed because it provided faster alignment times (independent alignment of pump and signal) and allowed an easier assessment of the injected signal value.

The pump laser was a JDSU-63-00352-20/AKU944 (10 W,  $100\ \mu\text{m}$ ). In order to have a precise tuning of the laser emission at the  $\text{Yb}^{3+}$  ion peak absorption ( $\lambda = 976\ \text{nm}$ ), a Peltier module and a thermistor were employed to form a closed-loop temperature control of the laser. The laser beam was elliptical, having two different divergences ( $35^\circ$  for the fast axis and  $10^\circ$  in the slow axis) as a result of the laser's rectangular aperture. A cylindrical lens was placed at the output of the laser to reduce the divergence of the laser beam in one direction, thus resulting in a circular beam.

The pump laser beam was first focused and collimated by lens #1 (EdmundOptics #45-768 with  $\text{NA} = 0.1$ ,  $f = 60\ \text{mm}$ ,  $\varphi = 12\ \text{mm}$ ). The formed beam passed then through a beam shifter (3 mm transparent glass) that pre-compensates the axial displacement produced by the presence of the dichroic mirror. The pump beam became therefore centered and ready to be focused by lens #2 (EdmundOptics #65-436 with  $\text{NA} = 0.4$ ,  $f = 15\ \text{mm}$ ,  $\varphi = 12\ \text{mm}$ ) into a small spot at point Q (working point). Both lenses provided a magnification ratio 1:4 to reduce the laser mode ( $100\ \mu\text{m}$ ) to the fiber cladding one ( $25\ \mu\text{m}$ ).

A tunable laser (Phonetics TUNICS) provided the signal power that was injected into the active fiber through a WDM combiner, which acted as an isolator to protect the tuning laser. The amplified signal was directly retrieved by using the integrating sphere at point F, as reported in figure 3. A filter



**Figure 3.** Experimental setup used for the  $\text{Yb}^{3+}\text{-Er}^{3+}$  fiber amplifier characterization in cladding-pumped configuration. Enclosed circled letters indicate measurement points used for the alignment and characterization of the setup. The two different paths followed by the pump and signal beams are shown in blue and red, respectively.

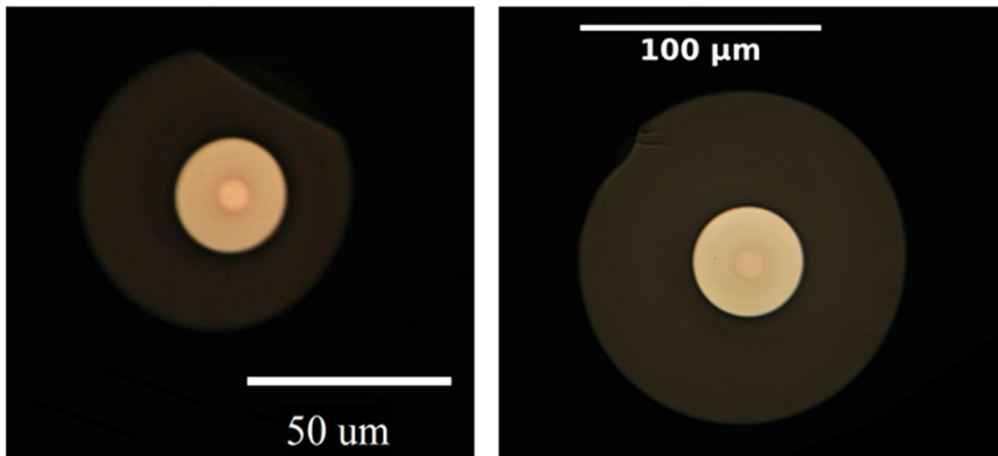


**Figure 4.** Transversal section of fibers A and B. (a) Fiber A:  $\Phi_{\text{core}} = 7 \mu\text{m}$ ,  $\Phi_{\text{inner clad}} = 25 \mu\text{m}$ ,  $\Phi_{\text{outer clad}} = 70 \mu\text{m}$ ,  $\text{NA}_{\text{core}} = 0.17$ ,  $N_{\text{clad}} = 0.44$ . (b) Fiber B:  $\Phi_{\text{core}} = 12 \mu\text{m}$ ,  $\Phi_{\text{inner clad}} = 48 \mu\text{m}$ ,  $\Phi_{\text{outer clad}} = 140 \mu\text{m}$ ,  $\text{NA}_{\text{core}} = 0.08$ ,  $N_{\text{clad}} = 0.4$ .

(Thorlabs FEL 1100) was inserted to avoid false readings due to the residual pump power.

### 3. Results and discussion

#### 3.1. Fiber characterization

Optical micrographs of fibers A and B sections are shown in figure 4, where the triple glass structure, featuring the Yb-Er doped glass core in the center, is clearly evident.

The near-field images of manufactured active fibers were measured at 1300 nm in order to evaluate the guiding properties of the fibers. The light beam was well confined inside the active area of the fiber, and only a negligible diffused area was observed inside the inner cladding.

Fiber losses were measured using a cut-back technique as explained in section 2.1. The obtained attenuation coefficients

were  $7.1 \pm 0.1 \text{ dB m}^{-1}$  and  $4.1 \pm 0.1 \text{ dB m}^{-1}$  for fibers A and B, respectively. Losses are mainly due to absorption and scattering effects, in particular at the interface between the core and first cladding. This could also explain why fiber A presents higher losses than fiber B, although the material and the fabrication process are essentially the same. In fiber A, due to the smaller core, the signal mode penetrates more into the first clad, and therefore its propagation is much more affected by the presence of absorption and scattering centers at the interface.

#### 3.2. Core-pumped amplifier demonstration

Optical amplification in a core-pumped configuration was demonstrated using  $27 \pm 2 \text{ mm}$  of fiber type A, with the setup depicted in figure 2.

Net gain was achieved for signal wavelength ranging from 1527 nm up to 1549 nm and signal powers from

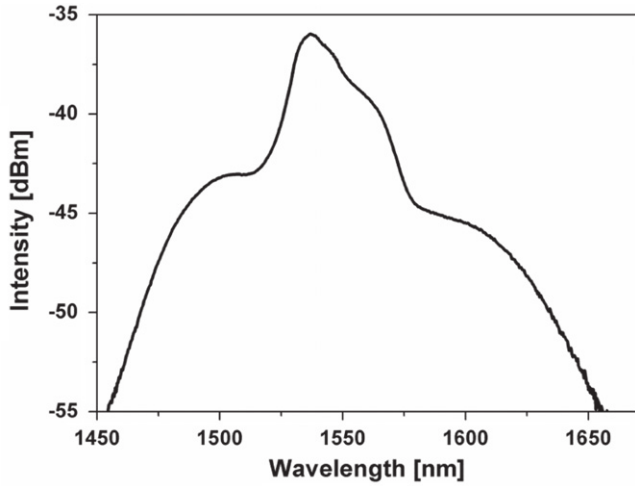


**Figure 5.** Amplified spontaneous emission (ASE) of 8 cm of fiber type B, when pumped at 976 nm.

–30 dBm up to 0 dBm. Considering internal gain rather than net gain, the wavelengths for which the fiber effectively acted as an amplifier ranged from 1515 nm up to about 1575 nm.

A maximum internal gain of  $10.7 \pm 0.7$  dB was obtained with the minimum input signal (–30 dBm) and a 479 mW pump power. This leads to an internal gain per unit length of  $4.0 \pm 0.1$  dB  $\text{cm}^{-1}$ , a value that is higher than values reported in [22, 23] and comparable to the values reported in [24, 25] ( $4.2$  dB  $\text{cm}^{-1}$  and  $5.2$  dB  $\text{cm}^{-1}$ ).

Detailed description and discussion of gain measurement results in core-pumped configuration can be found in [26].

The intense visible green emission arising from the fiber during measurements suggested that the pumping efficiency was limited by an upconversion mechanism. The green luminescence was shown to increase with increasing pump power.

The spectral quality of the green luminescence was analyzed using an OceanOptics USB2000+ spectrometer. The light coming from the amplifier's output (in the absence of input signal) was collimated using an X40 microscope. A shortpass filter FES750 was used to eliminate possible residual pump.

Although the luminescence looks green, the analysis showed some amount of red content. The green peaks bar-center wavelengths (530 nm and 550 nm) match the corresponding emission wavelengths of the  $\text{Er}^{3+}$  energy levels  $^2\text{H}_{11/2}$  and  $^4\text{S}_{3/2}$ , while the red peak (670 nm) is in agreement with the  $^4\text{F}_{9/2}$  one [27]. The population of these upper excitation levels is due to concentration quenching of  $\text{Er}^{3+}$  ions in glass that is believed to be dominated by cooperative up-conversion processes [28].

### 3.3. Cladding-pumped amplifier demonstration

At first, optical amplification in the counter-propagating cladding-pumped configuration was demonstrated using  $8.0 \pm 0.2$  cm of fiber type B, with the setup depicted in figure 3.

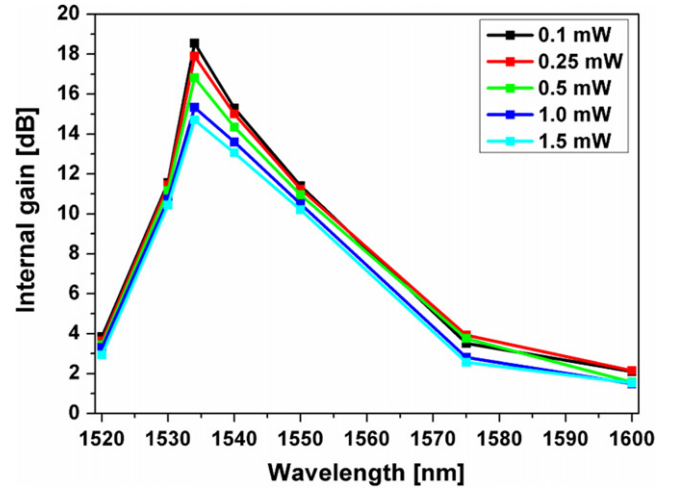


**Figure 6.** Internal gain spectra of the cladding-pumped amplifier realized with fiber B. Measurements were collected for five different signal input powers of 0.1 mW, 0.25 mW, 0.5 mW, 1 mW e 1.5 mW at wavelengths ranging from 1520 nm to 1600 nm. Injected pump power was estimated to be 1640 mW at 976 nm.

Amplified spontaneous emission (ASE) of the fiber, when pumped at 976 nm, is reported in figure 5.

The amplified signal (available at working point F) was measured for five different signal input powers of 0.1, 0.25, 0.5, 1 and 1.5 mW at wavelengths ranging from 1520 nm to 1600 nm. These measurements allowed computing the internal gain, i.e., the amplifier gain between point Q and T; the obtained results are reported in figure 6.

The amplifier reached a maximum signal output power of 48.9 mW for an injected input signal of 1.3 mW and 1640 mW pump power.

The maximum gain of  $18.5 \pm 0.7$  dB was reached for an input signal of 0.1 mW, resulting in a gain per length of  $2.3 \pm 0.1$  dB  $\text{cm}^{-1}$ , a value that is comparable to the one reported in [29].

The internal gain as a function of pump power was not measurable, since the laser current could not be modified more than 0.7 A without being out of the peak wavelength (976 nm).

The amplifier was rotated  $180^\circ$  (end-facets were inverted) and similar behavior was observed.

A length of  $8.0 \pm 0.2$  cm of fiber A (small fiber type) was tested for amplification using the counter-propagating cladding-pumped setup depicted in figure 3. It provided the highest output power (105 mW) but operated as a laser. It is believed that this was the result of having a high gain value combined with a random cleaving condition that led to the formation of a resonance cavity. It can be calculated that a round-trip gain of 27 dB is required in order to surpass the losses produced by Fresnel reflection at each amplifier fiber end combined with the amplifier losses (0.4 dB for a 10 cm length). This supposes a 14 dB single-pass gain, which is a value that has already been observed in other amplifiers.

In order to avoid the lasing condition by introducing some losses, a longer length of fiber A was tested in the counter-propagating cladding-pumped setup. Optical

amplification was demonstrated using 12 cm of fiber A. This amplifier reached a maximum gain of  $17.8 \pm 0.7$  dB, providing the highest recorded signal output power of 78.7 mW using an injected input signal of 1.3 mW, which was the highest available. The efficiency of this amplifier was 4.8%, considering that the injected pump power was 1640 mW. The gain per unit length was  $1.5 \pm 0.1$  dB cm<sup>-1</sup>.

#### 4. Conclusion

Two high concentration Yb-Er co-doped DC optical fibers (named A and B for short), based on in-house-developed phosphate glasses, were successfully drawn and characterized with the aim of engineering compact fiber optical amplifiers.

Fiber A (7/25/70 μm; NA=0.17) was evaluated in a core-pumped condition using a commercial WDM combiner. A maximum  $4.0 \pm 0.1$  dB cm<sup>-1</sup> gain per unit length was obtained for a -30 dBm signal at 1535 nm and 479.8 mW pump power. Both fibers A and B were used to demonstrate optical amplification in a counter-propagating cladding-pumped configuration. Using 8 cm of fiber B (12/48/140 μm and NA=0.08), a maximum internal gain of  $18.5 \pm 0.7$  dB was reached, for small signal input at 1535 nm, resulting in a gain per length of  $2.3 \pm 0.1$  dB cm<sup>-1</sup>.

This preliminary study showed that the developed high dopant concentration phosphate glass fibers offer the potential for high gain per length coefficients, allowing the realization of compact active devices. In particular, these phosphate-based fibers can be employed for the realization of pulsed fiber amplifiers for a MOPA system that maximizes energy extraction and minimizes nonlinear effects, thanks to the short length of interaction. Furthermore, phosphate glass fibers can be also spliced to silica-based components with low loss and high strength, enabling the realization of a monolithic all-fiber MOPA system with true potential for out-of-the lab exploitation.

In order to improve fiber amplification, future efforts will be devoted to the enhancement of the glass composition (in order to eliminate detrimental effects such as up-conversion, OH<sup>-</sup> groups inclusions, etc), optimization of the ratio of Yb<sup>3+</sup>/Er<sup>3+</sup> ions doping concentration and improvement of fiber manufacturing technique (reducing contaminations and enhancing sharpness at the glass interfaces).

#### Acknowledgments

This work was supported by the Vinci project 'Programma Vinci 2010—Cap. III' Italian- French University Research Training program and by Eurostars—Project E!6174 SIMPLE.

#### References

- [1] Richardson D J, Nilsson J and Clarkson W A 2010 High power fiber lasers: current status and future perspectives *J. Opt. Soc. Am. B* **27** B63–92
- [2] Liem A, Limpert J, Zellmer H and Tünnermann A 2003 100 W single-frequency master-oscillator fiber power amplifier *Opt. Lett.* **28** 1537–9
- [3] Wang L, He D, Feng S, Yu C, Hu L, Qiu J and Chen D 2014 Yb/Er co-doped phosphate ar *Sci. Rep.* **4** 6139
- [4] Ogino J, Sueda K, Kurita T, Kawashima T and Miyanaga N 2013 High-gain regenerative chirped-pulse amplifier using photonic crystal rod fiber *Appl. Phys. Express.* **6** 122703
- [5] Gu G, Kong F, Hawkins T, Parsons J, Jones M, Dunn C, Kalichevsky-Dong M, Saitoh K and Dong L 2014 Ytterbium-doped large-mode-area all-solid photonic bandgap fiber lasers *Opt. Express* **22** 13962–8
- [6] Izumitani T S 1986 *Optical Glass* (New York: American Institute of Physics) pp 162–72
- [7] Lee Y-W, Sinha S, Dignonnet M J F, Byer R L and Jiang S 2006 20 W single-mode Yb<sup>3+</sup>-doped phosphate fiber laser *Opt. Lett.* **31** 3255–7
- [8] Campbell J H 1996 Recent advances in phosphate laser glasses for high-power applications *Proc. SPIE CR64, Inorganic Optical Materials (Riga, July)* pp 3–39
- [9] Lee Y-W, Dignonnet M J F, Sinha S, Urbanek K E, Byer R L and Jiang S 2009 High-power Yb<sup>3+</sup>-doped phosphate fiber amplifier *J. Sel. Top. Quant. Electron.* **15** 93–102
- [10] Gapontsev V P, Matitsin S M, Isineev A A and Kravchenko V B 1982 Erbium glass lasers and their applications *Opt. Laser Technol.* **14** 189–96
- [11] Hwang B-C, Jiang S, Luo T, Watson J, Sorbello G and Peyghambarian N 2000 Cooperative upconversion and energy transfer of new high Er<sup>3+</sup>- and Yb<sup>3+</sup>-Er<sup>3+</sup>-doped phosphate glasses *J. Opt. Soc. Am. B* **17** 833–9
- [12] Hu Y, Jiang S, Luo T, Seneschal K, Morrell M, Smektala F, Honkanen S, Lucas J and Peyghambarian N 2001 Performance of high-concentration Er<sup>3+</sup>-Yb<sup>3+</sup>-codoped phosphate fiber amplifiers *IEEE Photonics Technol. Lett.* **13** 657–9
- [13] Jiang S 2003 Erbium-doped phosphate fiber amplifiers *Proc. SPIE 5246, Active and Passive Optical Components for WDM Communications III (San Diego, March 2003)* pp 201–7
- [14] Spiegelberg C, Geng J, Hu Y, Kaneda Y, Jiang S and Peyghambarian N 2004 Low-noise narrow-linewidth fiber laser at 1550 nm *J. Lightwave Technol.* **22** 57–62
- [15] Qiu T, Suzuki S, Schülzgen A, Li L, Polynkin A, Temyanko V, Moloney J V and Peyghambarian N 2005 Generation of watt-level single-longitudinal-mode output from cladding-pumped short fiber lasers *Opt. Lett.* **30** 2748–50
- [16] Li L *et al* 2004 Short cladding-pumped Er/Yb phosphate fiber laser with 1.5 W output power *Appl. Phys. Lett.* **85** 2721–3
- [17] Hofmann P, Voigtländer C, Nolte S, Peyghambarian N and Schülzgen A 2013 550 mW output power from a narrow linewidth all-phosphate fiber laser *J. Lightwave Technol.* **31** 756–60
- [18] Vienne G G, Caplen J E, Dong L, Minelly J D, Nilsson J and Payne D 1998 Fabrication and characterization of Yb<sup>3+</sup>:Er<sup>3+</sup> phosphosilicate fibers for lasers *J. Lightwave Technol.* **16** 1990–2001
- [19] Akbulut M, Miller A, Wiersma K, Zong J, Rhonehouse D, Nguyen D and Chavez-Pirson A 2014 High energy, high average and peak power phosphate-glass fiber amplifiers for Imicron band *Proc. SPIE 8961, Fiber Lasers XI: Technology, Systems, and Applications* **8961** 89611X

- [20] Chavez-Pirson A 2010 Highly doped phosphate glass fibers for fiber lasers and amplifiers with applications *Proc. SPIE* **7839**, *2nd Workshop on Specialty Optical Fibers and Their Applications (WSOF-2) (Oaxaca, October)* 78390K
- [21] Peng X *et al* 2013 High efficiency, monolithic fiber chirped pulse amplification system for high energy femtosecond pulse generation *Opt. Express* **21** 25440–51
- [22] Shi W, Leigh M, Zong J, Yao Z and Jiang S 2008 Photonic narrow linewidth GHz source based on highly codoped phosphate glass fiber lasers in a single MOPA chain *IEEE Photonics Technol. Lett.* **20** 69–71
- [23] Xu S H, Yang Z M, Feng Z M, Zhang Q Y, Jiang Z H and Xu W C 2008 Gain and noise characteristics of single-mode Er<sup>3+</sup>/Yb<sup>3+</sup> Co-doped phosphate glass fibers *Proc. 2nd IEEE International Nanoelectronics Conf. (INEC 2008) (Shanghai, March)* pp 633–5
- [24] Pan Z, Xu Q, Meng L, Cai H, Fang Z and Qu R 2009 Single-polarization operation of phosphate fiber laser induced by external feedback *Proc. 8th Pacific Rim Conf. on Lasers and Electro-Optics (CLEO/Pacific Rim 2009) (Shanghai, September)* pp 1249
- [25] Xu S H, Yang Z M, Liu T, Zhang W N, Feng Z M, Zhang Q Y and Jiang Z H 2010 An efficient compact 300 mW narrow-linewidth single frequency fiber laser at 1.5  $\mu\text{m}$  *Opt. Express* **18** 1249–54
- [26] Scarpignato G C, Milanese D, Lousteau J, Boetti N G and Mura E 2013 Fabrication and characterization of a high-gain Yb-Er codoped phosphate glass optical amplifier *J. Engineering* **2013** 858341
- [27] Dignonnet M J F 2001 *Rare-Earth-Doped Fiber Lasers and Amplifiers* 2nd ed (New York: Marcel Dekker)
- [28] Miniscalco W J 1991 Erbium-doped glasses for fiber amplifiers at 1500 nm *J. Lightwave Technol.* **9** 234–50
- [29] Nguyen D T, Chavez-Pirson A, Jiang S and Peyghambarian N 2007 A novel approach of modeling cladding-pumped highly Er–Yb co-doped fiber amplifiers *IEEE J. Quantum Electron.* **43** 1018–27